ISSN: 2350-0328
International Journal of Advanced Research in Science, Engineering and Technology
Vol. 7, Issue 5 , May 2020

Investigation of Water Sorption to Ca_5Na_3A Zeolite at Adsorption of Micro Calorimetric Device

Kokharov Mirzokhid Husanboevich, Axmedov Ulug' Karimovich, Rakhmatkarieva Firuza Gayratovna, Abduraxmonov Eldor Baratovich.

PhD Student, Institute of General and Inorganic chemistry, Uzbek Academy of Sciences, Tashkent, Uzbekistan
Professor, Doctor of Chemical Sciences, Institute of General and Inorganic chemistry, Uzbek Academy of Sciences, Tashkent, Uzbekistan
Leading researcher Institute of General and Inorganic chemistry, Uzbek Academy of Sciences, Tashkent, Uzbekistan
PhD, Institute of General and Inorganic chemistry, Uzbek Academy of Sciences, Tashkent, Uzbekistan

ABSTRACT: Isotherm, differential heats, entropy and thermokinetics of water adsorption in Ca_5Na_3A A zeolite were measured at 303K. The detailed mechanism of water adsorption in Ca_5Na_3A zeolite from zero filling to saturation was discovered. The adsorption isotherm was quantitatively reproduced by the Theory for Volume filling of Micropores (TVFM) theory equations.

KEY WORDS: Isotherm, differential heats of adsorption, entropy, thermokinetics, ion-molecular complexes, zeolite Ca_5Na_3A, CO_2, adsorption calorimetry.

I. INTRODUCTION

Adsorption mainly involves the absorption of adsorbate molecules to the adsorbent surface. Adsorbent is usually a micronutrient with a high surface area. The adsorbate forms thin layers as a result of physical adsorption and chemical adsorption on the adsorbent surface. If the adsorbent effects of adsorbate are due to chemical bonds, then physical adsorption occurs if chemical adsorption occurs under the forces of van der Vaal's (1).
It is important to calculate adsorption enthalpies during heat release and cooling in adsorption gases [2-4], adsorption desalination [5-7] and adsorption of adsorbed molecules [8-16]. 13X [17] and the adsorption of N_2, O_2, and CO_2 molecules in CaA zeolites is based on calorimetric measurements by esoteric methods, and the esoteric method is required to determine the thermodynamic values required to calculate the differential energy of the adsorption process [18,19,20]. This method is used to study the physical adsorption of the adsorption process [21].
Adsorption enthalpies are calculated using calorimetric measurements using the Tian-Calve calorimeter [22] and esostatic enthalpy of adsorption.
Examining the adsorption properties of zeolites reveals their adsorption isotherm, thermodynamic, and kinetic functions [23-29].

II. RESEARCH METHODS AND OBJECTS

For micro calorimetric research, a type A synthetic Ca_5Na_3A zeolite (Si/Al=1) was used. The content of elemental cells of the zeolite obtained for the study is Ca_5Na_3A – Ca_5Na_3 $[(AlO_2)_{12}(SiO_2)_{12}]$ $27H_2O$. Absolute water was selected for adsorption with Ca_5Na_3A zeolite. Ca_5Na_3A zeolite was carried out in a high-vacuum adsorption at micro calorimetric device for water adsorption detection [30-31].
The adsorbates were first frozen and then purified by vacuum pump and zeolite. The micro calorimeter allows measuring long-term heat energy. The adsorption measurements were performed on a high vacuum adsorption device and calculated by capillary method. Low adsorption of adsorbents increases the accuracy of adsorption measurements.

III. OBTAINED RESULTS AND DISCUSSIONS

The amount of adsorption (N) is expressed in the elemental cell (e.c) H_2O, and the isotherm is expressed in units of ln (p/p0). Figure 1 shows at the temperature at 303 K on Ca_5Na_3A zeolite of the water adsorption of isotherm is ln (p/p0)

ISSN: 2350-0328
International Journal of Advanced Research in Science, Engineering and Technology
Vol. 7, Issue 5 , May 2020

of (p0-water vapor pressure, p0 (303K) = 4,42 kPa) at a relative pressure of ~10-6. The adsorption isotherm was studied in three parts. In the first section, the adsorption isotherm of water in Ca_5Na_3A zeolite is initially ln (p/p°)=-16,74, p-0.00000171 millimeters of mercury, and the adsorption rate begins at N = 0,265 H_2O/e.c. Adsorption isotherm ln (p/p°)=-16,74 to ln (p/p°)=-10,06, towards the adsorption axis, where the adsorption rate will be N=10,19 H_2O/e.c. Here the adsorption pressure is in the range of p-0.00000171 mm. over thermometer from p-0.0011358 mm. over thermometer. At the same time, the adsorption and isotherm values and graphs show that water molecules are firmly in the zeolite pores, and the adsorbate molecules are inactive. In the second part, the adsorption isotherm rises vertically until it reaches ln (p/p°) =-10,19 and the adsorption reaches N=11,37 H_2O/e.c. In the third fragment, the isotherm is partially bent towards the adsorption axis at ln (p/p°) =-10,06 to ln (p/p°) =-4.43, where the adsorption rate is N=19,85 H_2O/e.c equals this. The atmospheric pressure at these ranges is r-0.001358 mm over thermometer from p-0.38 mm over thermometer.

Adsorption of water molecules is also strongly enhanced at this stage, that is, it forms complexes with metal cations contained in zeolite. The metal cations in the zeolite pores with water molecules form complex compounds in the first and second stages.

Then, in the third section, the isothermal signs rise partially vertically from ln (p/p°)=-4,43 to ln (p/p°) = - 0,1, and adsorption will be around N=19, 85 H_2O/e.c and N = 35,91. H_2O/e.c. At the end of the process, the adsorption atmospheric pressure is p-28,71 mm over thermometer and water saturation approaches the vapor pressure.

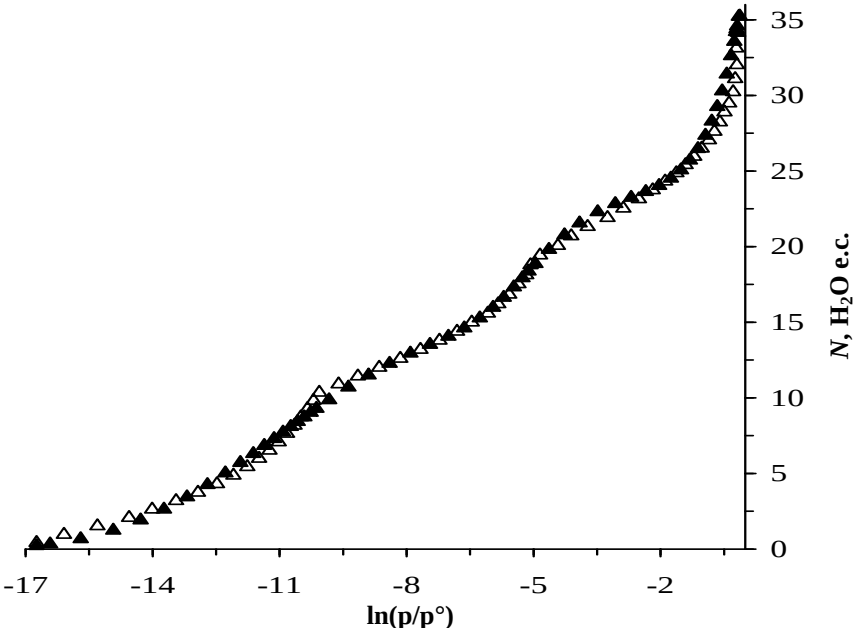

Figure 1. Water adsorption isotherm in the zeolite Ca_5Na_3A at 303K.
Δ-experimental data. ▲- estimating data by VMOT

Adsorption isotherm of water in the Ca_5Na_3A zeolites is sat-isfactorily described by three term equation of the the-ory of volumetric micropore occupancy (VMOT) [32-33].

$N = 15{,}835\exp[A/30{,}03)^4]+7{,}406\exp[A/13{,}32)^5]+14{,}765\exp[A/1{,}89)^1]$,

Where: N-adsorption in microwaves, (H_2O/e.c, A=RTln (P°/P) –1 H_2O/e.c (P° pressure) to transport vapor from surface (P° pressure) to a gas phase.

Figure 2 shows the differential heat (Q_d) adsorption of water to Ca_5Na_3A zeolite at a temperature of 303 K. Long lines-heat condensation of water below 303 K (ΔH_v=43,5 кJ/mol). In this zeolite, the adsorption heat decreases in the form of a wave-like step. Adsorption generates several small steps. At the first stage, the adsorption of water molecules on Ca_5Na_3A zeolite (starting at N=0,29 H_2O/e.c) starts with a differential heat of~106,42 kJ/mol. Subsequently, adsorption with differential heat up to N = 3.02 H_2O/e.c and gradually decreases to Q_d -81,39 kJ / mol. The adsorption heat is Q_d-98,23kJ/mol when adsorption is N = 0,806 H_2O/e.c. The high heat of adsorption here is due to the fact that water molecules penetrate into the zeolite cavities because of their small size and the oxygen atoms joining silicon aluminum

ISSN: 2350-0328
International Journal of Advanced Research in Science, Engineering and Technology
Vol. 7, Issue 5 , May 2020

at the entrance. Here again, the cations in the zeolite microwaves are inactive until water molecules are distributed. Then the adsorption N = 3,02 H_2O/e.c decreases sequentially to Q_d = 81,39 kJ/mol. Then, N = 3,02 H_2O/e.c N = 5,819 H_2O/e.c forms a second high-energy second low adsorption interval (where Q_d = 81,39 kJ/mol).
The main reason for the orderly step reduction from the second step is the formation of complex compounds with metal cations located in active centers in the zeolite pores.
The adsorption is the third smallest in the range N = 5,819 to 9,116 H_2O/e.c (Q_d = 74,79 kJ/mol). The second and third steps are 2,799 H_2O/e.c and 3,297 H_2O/e.c. At this stage, the adsorption heat gradually decreases from 81.39 kJ/mol to 71,49 kJ/mol. The difference between the adsorption heats is ~ 10 kJ/mol. The fourth N = 9,116 H_2O/e.c is 11,82 H_2O/e.c and the fifth sub-step is followed by two spots in the interval from 11,82 to 14,20 H_2O/e.c. At these stages, the adsorption heat decreases from 71,49 kJ/mol to 66.55 kJ/mol in the fourth step and to 64,0 kJ/mol in the fifth step. The fourth and fifth steps are 2,704 H_2O/e.c and 2.38 H_2O/e.c. If it counts for the adsorption quantities of the four small steps above contain two large steps. Large steps showed a decrease in adsorption heat from 81.39 kJ/mol to 71,49 kJ/mol. In the processes that go with high adsorption heat, S_{III} occurs in pores. In the case of type A S_{II}, the adsorption heat decreases in a uniform waveform.
In addition, when the adsorption at the sixth step reaches 14,20, there is a gradual decrease in the differential heat, and the differential heat decreases from 64,0 kJ/mol to 62,04 kJ/mol. Then the adsorption temperature will be the seventh small step from 62,04 kJ/mol to 58,43 kJ/mol. The adsorption range is 1,92 H_2O/e.c, and the heat range is 3.61 kJ/mol. The amount of adsorption decreases in the range from 19,21 H_2O/e.c to 29,96 H_2O/e.c with a differential temperature from 58,43 kJ/mol to 44,79 kJ/mol. At these adsorption intervals, three smaller steps are formed. These are eighth in the range from 19,21 H_2O/e.c to 22,94 H_2O/e.c, the ninth in the low 22,94 H_2O/e.c and the lowest tenth in 26,32 H_2O/e.c is 29,96 H_2O/e.c.

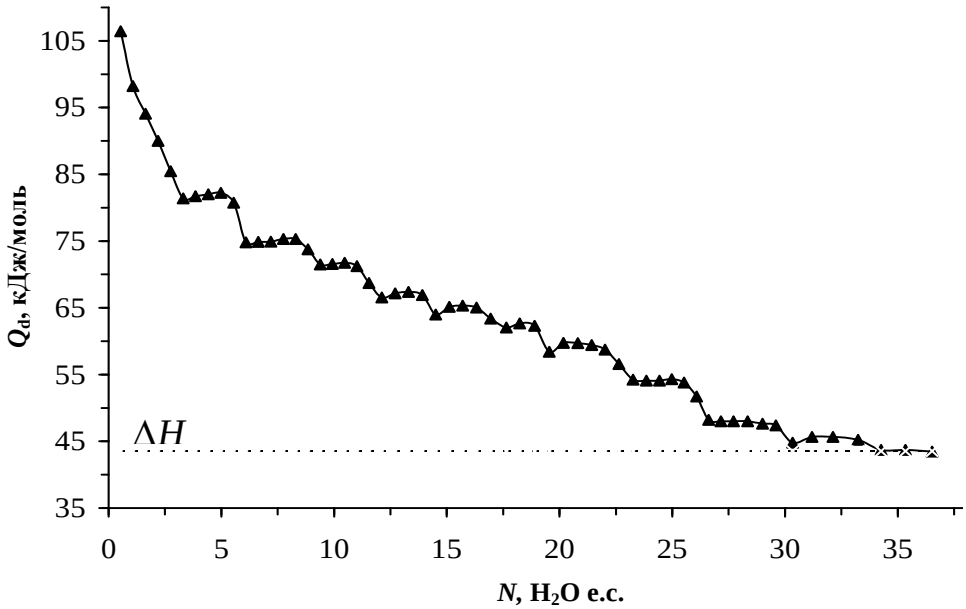

Figure 2 The differential heat of water adsorption in the zeolite Ca_5Na_3A at 303K.
The horizontal dashed line is heat water condensation at 303K

After these steps, the heat of adsorption approaches the condensation heat. The process ends with two more steps. In the eleventh step, the adsorption rates range from 29,96 H_2O/e.c to 33.75 H_2O/e.c (Q_d = 44,79 kJ/mol to 43,54 kJ/mol) and the twelfth step to 33.75 H_2O / eya, reaching 35, 93 H_2O/e.c. The adsorption of Na^+ and Ca_2^+ cations in the zeolite pore ranges from 9,116 H_2O/cell to 26.32 H_2O/e.c cells. At this stage, 17,204 H_2O/e.c water molecules are adsorbed into Na^+ and Ca^{2+} cations. At the same time, multivariate complexes $(H_2O)_nNa^+$ and $(H_2O)_nCa^{2+}$ are formed.
In the pore of the Ca_5Na_3A zeolite, there are 3 active centers, the adsorption cavities, where the adsorbates are adsorbed. Alkaline and alkaline earth metals are the basis of active centers. In the first cavity, the Ca^{2+} cations are located in the center of the S_I six-member oxygen ring and form the β-cavity. This cavity is partially saturated with metal cations

ISSN: 2350-0328
International Journal of Advanced Research in Science, Engineering and Technology
Vol. 7, Issue 5 , May 2020

because of its small size. In the second cavity, the Ca^{2+} and Na^{+} cations are located slightly inside the S_{II} eight-member oxygen ring plane and finally in the third cavity, the Ca^{2+} cations is in the large α-cavity opposite the S_{III} quadruple oxygen ring.

Apparently, S_{III} and S_{II} cavities constitute the bulk of the adsorption because they are located within the super cavity. Because the cations in the S_I cavity are poorly adsorbed because they are surrounded by cations of six strong oxygen atoms. A total of 35.93 H_2O/e.c per Ca_5Na_3A eya water molecules are adsorbed. Of these, ~26.94 H_2O/e.c in the S_{II} cavity, and S_{III} cavity is ~8,184 H_2O/e.c. The S_I cavity space is 0.806 e.c.

The Gibbs-Helmholtz equation was used to calculate the differential entropy using the differential heat of water adsorption and the isotherm values for Ca_5Na_3A zeolite [9].

$$\Delta S_{\mathrm{d}} = \frac{\Delta H - \Delta G}{T} = \frac{-(Q_{\mathrm{d}} - \lambda) + A}{T}$$

λ-thermal condensation, ΔH and ΔG-enthalpy and free energy change, T - temperature, Q_d ´-middle differential heat.

Figure 3 shows the differential entropy of water adsorption to Ca_5Na_3A zeolite. It is clear from the beginning of the process that the adsorption heat is high, indicating that at the initial saturation, the water molecules are not in a tight state of the zeolite microbes.

Shows adsorption differential entropy initially begins at -54.88 J/mol*K, where the adsorption is N = 0.53 H_2O/e.c. Then the entropy decreases to -13.72 J / mol*K and there is an increase of -24.77 J/mol*K. In this part of the zeolite, there is an abundance of free pore space, and the aluminum and silicon oxides that form it are highly energized by the contact of water molecules to the oxygen atoms.

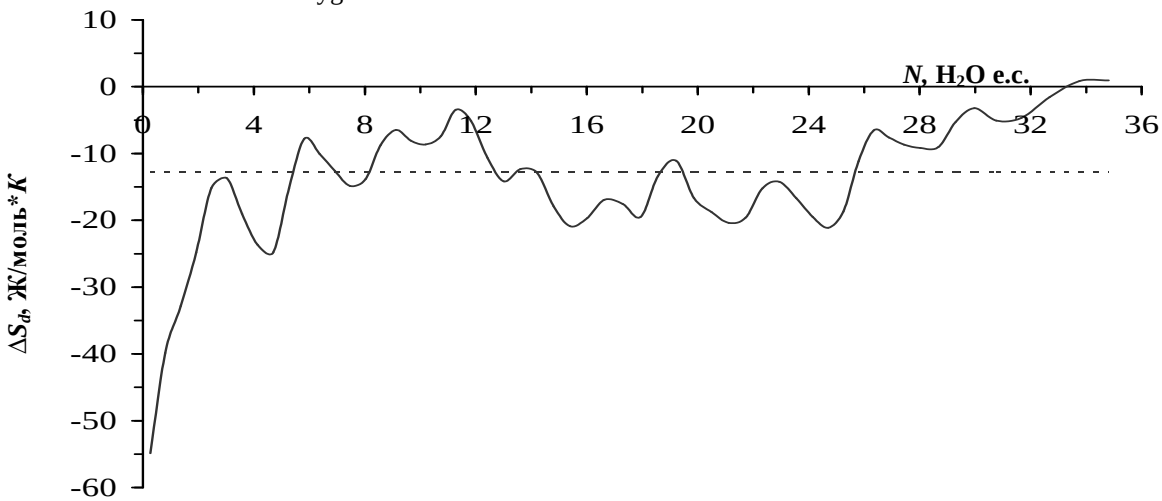

Figure 3. The differential entropy of the water adsorption in the zeolite Ca_5Na_3A at 303K. Entropy of liquid water is taken as zero. The horizontal dashed line – mean molar integral entropy.

The adsorption differential entropy is wave-shaped, rising from N = 4.98 H_2O/e.c to N = 15,69 H_2O/e.c with wave lines at -20,90 J/mol*K. Adsorption goes below the mean integral entropy line from N = 15,69 H_2O/e.c to N = 24.98 H_2O/e.c. The adsorption is then gradually slotted over the mean integral lines after N = 24.98 H_2O/e.c and approaches 0. This is adsorbed to the S_{II} cavities of the zeolite matrix while forming small waveforms. Due to the large number of cations in these cavities, the distribution of energy in cations migration and adsorption is regular and strongly adsorbed. The mean integral entropy is -12.75 J/mol*K.

Figure 4 shows the equilibrium time of water adsorption to Ca_5Na_3A zeolite. In this zeolite the equilibrium time curves are strongly.

Shows the adsorption time of water adsorption to Ca_5Na_3A zeolite is initially 26.18 h. In the initial saturation process, the water adsorption takes longer to stabilize. This may be explained by the fact that the distribution of water molecules in the cations of the zeolite and cations in the pore space takes longer. Basically, when the adsorption is up to N ~ 25.19 H_2O/e.c, the equilibrium time curves are in the form of a strong wave. After that, the equilibrium time gradually

ISSN: 2350-0328
International Journal of Advanced Research in Science, Engineering and Technology
Vol. 7, Issue 5 , May 2020

decreases for several hours. The differential heat of water adsorption to Ca_5Na_3A zeolite is in the form of a small step, which can be observed even during equilibrium.

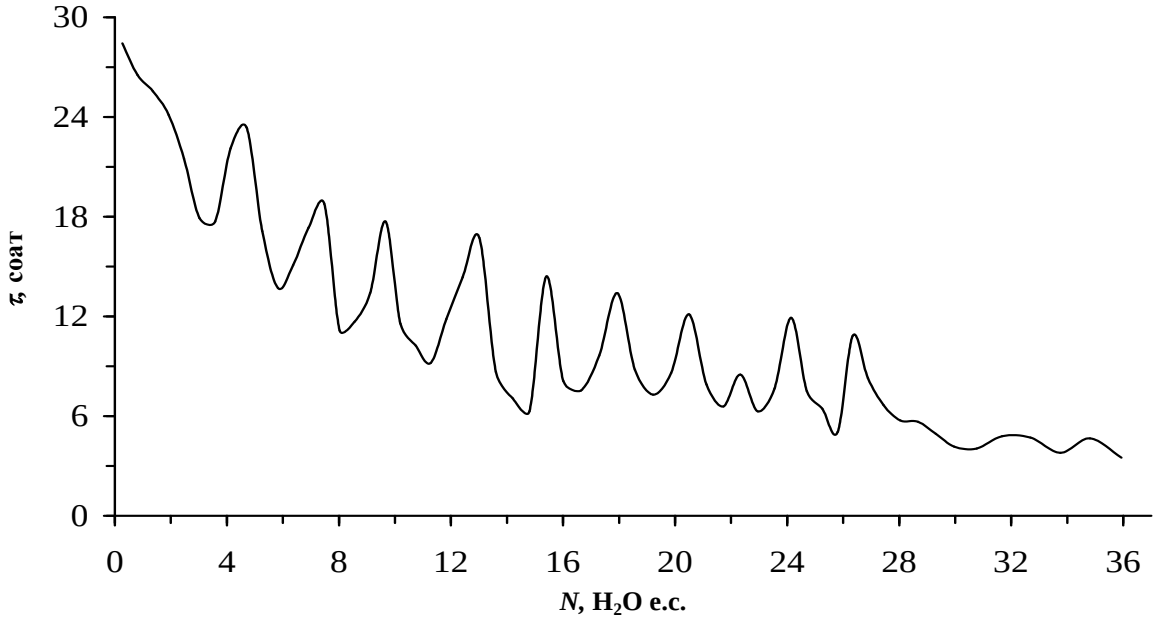

Figure 4.–The set-time of the adsorption equilibrium, depending on the size of the adsorption of water in the zeolite Ca_5Na_3A at 303K.

IV. CONCLUSION

The adsorption heat of the water in the Ca_5Na_3A zeolites is of a small footprint, where all steps form the single and multi-dimensional adsorption complexes $(H_2O)_n/Ca^+$ and $(H_2O)_n/Na^+$ in Ca_5Na_3A zeolite. The adsorption isotherm is represented by a three-axis micro size adsorption of the theory equation. The total sorption capacity of the Ca_5Na_3A zeolite is about ~3636.53 H_2O/e.c water molecules. On the basis of the differential entropy values, water molecules are strongly adsorbed to these zeolite microbes. The adsorption differential entropy has average integral entropy of -12,75 J/mol*K. Water molecules are strongly adsorbed in solid state in the zeolite superpowers. The adsorption of water to Ca_5Na_3A zeolite initially starts at 28,44 hours and is reduced to several hours (3.4 hours) at the end of the process.

REFERENCES

[1]. Kapil Narwal, R. Kempers, P. G. O'Brien. Adsorbent-Adsorbate Pairs for Solar Thermal Energy Storage in Residential Heating Applications: A Comparative Study // Proceedings of The Canadian Society for Mechanical Engineering International Congress 2018 May 27-30, 2018, Toronto, On, Canada
[2]. Fracaroli A. M. *et al.* Metal–organic frameworks with precisely designed interior for carbon dioxide capture in the presence of water. Journal of the American Chemical Society 136, 8863–8866 (2014).
[3]. Gándara F., Furukawa H., Lee S. & Yaghi O. M. High Methane Storage Capacity in Aluminum Metal–Organic Frameworks. Journal of the American Chemical Society 136, 5271–5274 (2014)
[4]. Nguyen N. T. et al. Selective Capture of Carbon Dioxide under Humid Conditions by Hydrophobic Chabazite-Type Zeolitic Imidazole Frameworks. Angewandte Chemie 126, 10821–10824 (2014).
[5]. Ng K. C., Thu K., Kim Y., Chakraborty A. & Amy G. Adsorption desalination: an emerging low-cost thermal desalination method. Desalination 308, 161–179 (2013).
[6]. Thu K., Ng K. C., Saha B. B., Chakraborty A. & Koyama S. Operational strategy of adsorption desalination systems. International Journal of Heat and Mass Transfer 52, 1811–1816 (2009).
[7]. Wu J. W., Hu E. J. & Biggs M. J. Thermodynamic cycles of adsorption desalination system. Applied Energy 90, 316–322 (2012).
[8]. Aristov Y. I. Novel materials for adsorptive heat pumping and storage: screening and nanotailoring of sorption properties. Journal of Chemical Engineering of Japan 40, 1242–1251 (2007)

ISSN: 2350-0328
International Journal of Advanced Research in Science, Engineering and Technology
Vol. 7, Issue 5 , May 2020

[9]. El-Sharkawy I. I. *et al.* Adsorption of ethanol onto phenol resin based adsorbents for developing next generation cooling systems. International Journal of Heat and Mass Transfer 81, 171–178 (2015).
[10]. Golubovic M. N., Hettiarachchi H. & Worek W. M. Sorption properties for different types of molecular sieve and their influence on optimum dehumidification performance of desiccant wheels. International Journal of Heat and Mass Transfer 49, 2802–2809 (2006).
[11]. Henninger S., Schmidt F. & Henning H.-M. Water adsorption characteristics of novel materials for heat transformation applications. Applied thermal engineering 30, 1692–1702 (2010).
[12]. Narayanan S., Yang S., Kim H. & Wang E. N. Optimization of adsorption processes for climate control and thermal energy storage. International Journal of Heat and Mass Transfer 77, 288–300 (2014).
[13]. Henninger S. K., Habib H. A. & Janiak C. MOFs as adsorbents for low temperature heating and cooling applications. Journal of the American Chemical Society 131, 2776–2777 (2009).
[14]. Henninger S. K., Jeremias F., Kummer H. & Janiak C. MOFs for use in adsorption heat pump processes. European Journal of Inorganic Chemistry 2012, 2625–2634 (2012).
[15]. Narayanan S. *et al.* Thermal battery for portable climate control. Applied Energy 149, 104–116 (2015).
[16]. Canivet J., Fateeva A., Guo Y., Coasne B. & Farrusseng D. Water adsorption in MOFs: fundamentals and applications. Chemical Society Reviews 43, 5594–5617 (2014).
[17]. Shen, D., Below, M., Siperstein, F., Engelhard, M. & Myers, A. L. Comparison of experimental techniques for measuring isosteric heat of adsorption. Adsorption 6, 275–286 (2000).
[18]. Furukawa, H. et al. Water adsorption in porous metal–organic frameworks and related materials. Journal of the American Chemical Society 136, 4369–4381 (2014).
[19]. Kusgens, P. et al. Characterization of metal-organic frameworks by water adsorption. Microporous and Mesoporous Materials 120, 325–330 (2009).
[20]. Salame, I. I. & Bandosz, T. J. Experimental study of water adsorption on activated carbons. Langmuir 15, 587–593 (1999).
[21]. Li, X. et al. Zeolite Y adsorbents with high vapor uptake capacity and robust cycling stability for potential applications in advanced adsorption heat pumps. Microporous and Mesoporous Materials 201, 151–159 (2015).
[22]. Rouquerol, J., Rouquerol, F., Llewellyn, P., Maurin, G. & Sing, K. S. Adsorption by powders and porous solids: principles, methodology and applications. (Academic press, 2013).
[23]. P.S. Kumar, S. Ramalingam, C. Senthamarai, M. Niranjanaa, P. Vijayalakshmi, S. Sivanesan, Adsorption of dye from aqueous solution by cashew nut shell: studies on equilibrium isotherm, kinetics and thermodynamics of interactions, Desalination 261 (1–2) (2010) 52–60.
[24]. K.Y. Foo, B.H. Hameed, Insights into the modeling of adsorption isotherm systems, Chem. Eng. J. 156 (2010) 2–10.
[25]. H. Aydin, G. Baysal, Adsorption of acid dyes in aqueous solutions by shells of bittimpistacial khinjuk stocks Desalination 196 (2006) 248–259.
[26]. M.B. Desta, Batch sorption experiments: Langmuir and Freundlich isotherm studies for the adsorption of textile metal ions onto Teff straw (Eragrostis tef) agricultural waste, J. Thermodyn. 375830 (2013) 6, http://dx.doi.org/10.1155/2013/375830.
[27]. K.V. Kumar, A. Kumaran, Removal of methylene blue by mango seed kernel powder, Biochemistry. Eng. J. 27 (2005) 83–93.
[28]. C. Namasivayam, R.T. Yamuna, Adsorption of Chromium(VI) by a low-cost adsorbent: biogas residual slurry, Chemosphere 30 (1995) 561–578.
[29]. N.K. Hamadi, X.D. Chen, M.M. Farid, G.M. Lu, Adsorption kinetics for the removal of chromium(VI) from aqueous solution by adsorptions derived from used tires and sawdust, Chem. Eng. J. 84 (2001) 95–105.